

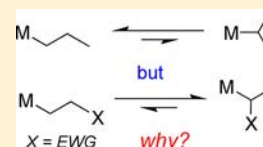
Rhodium–Carbon Bond Energies in Tp’Rh(CNneopentyl)(CH₂X)H: Quantifying Stabilization Effects in M–C Bonds

Yunzhe Jiao, Meagan E. Evans, James Morris, William W. Brennessel, and William D. Jones*

Department of Chemistry, University of Rochester, Rochester, New York 14627, United States

S Supporting Information

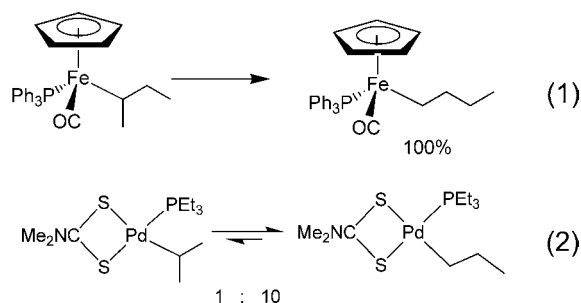
ABSTRACT: A series of substituted methyl derivatives of the type Tp’Rh(CNneopentyl)(CH₂X)H (CH₂X = CH₂C(=O)CH₃, CH₂C≡CCH₃, CH₂O-*t*-Bu, CH₂CF₃, CH₂F, CHF₂) was synthesized either by photolysis of Tp’Rh(CNneopentyl)(PhNCNneopentyl) in neat CH₃X or by exchange with the labile hydrocarbon in Tp’Rh(CNneopentyl)(*n*-pentyl)H or Tp’Rh(CNneopentyl)(CH₃)H. Only a single product was observed in each case. Clean reductive elimination was observed for all compounds in C₆D₆. Structures of these complexes and their corresponding chlorinated derivatives have been characterized by NMR spectroscopy, elemental analysis, and X-ray crystallography. Relative Rh–C bond energies are calculated using previously established kinetic techniques, and two separate linear correlations are observed versus known C–H bond strengths, one for the parent hydrocarbons, and one for the substituted hydrocarbons. Both correlations have slopes of 1.4, and are separated vertically by 7.5 kcal mol⁻¹ (–CH₂X above –C_xH_y). In addition, it is now clear that preferences for linear vs branched olefin insertion products in substituted derivatives can be predicted on the basis of the strengths of the β-C–H bonds. The DFT calculations of the metal–carbon bond strengths in these Rh–CH₂X derivatives with α-substitution show a trend that is in good agreement with the experimental results.



INTRODUCTION

One of the most important properties of homogeneous organometallic catalysts is their ability to control regioselectivity in alkene insertion reactions. For example, the hydroformylation of olefins by cobalt carbonyl shows preferential formation of linear over branched aldehydes (~4:1), and use of a bulkier rhodium catalyst can improve on this selectivity (~16:1).¹ Likewise, hydrocyanation of butadiene can be tailored to give as high as 98% linear addition product using a nickel diphosphine catalyst.² In these and other reactions, the kinetic and/or thermodynamic preferences for forming branched vs linear metal–alkyl bonds are critical to controlling the overall reaction selectivity. This in turn requires an understanding of relative metal–carbon bond strengths in a variety of substituted alkyl derivatives.

For the parent unsubstituted alkyl derivatives, there is strong evidence that the linear, primary metal–alkyl bond is preferred thermodynamically over the branched, secondary metal–alkyl bond. It was observed in the 1970s that hydrozirconation of isomers of octene led to the sole formation of the *n*-octylzirconium product.³ Kochi observed that a *tert*-butyl gold(III) complex isomerized spontaneously to the isobutyl isomer at 25 °C with a half-life of 17 h.⁴ Reger observed in 1980 that the secondary alkyl complex CpFe(CO)(PPh₃)(*sec*-butyl) rearranged quantitatively to the linear isomer upon heating to 63 °C (eq 1).⁵ A similar preference for the linear over the branched isomers was seen in a series of palladium–alkyl complexes at 75 °C (eq 2),⁶ and similar results were observed with platinum complexes at 130 °C.⁷ These and other observations^{8–10} of similar preferences, along with the corresponding reactivities of metal–alkyl carbonyls to undergo CO insertion,¹¹ have led to the general conclusion that a

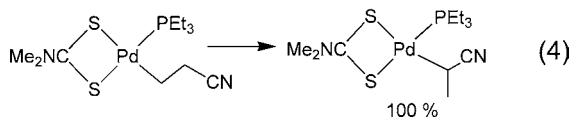
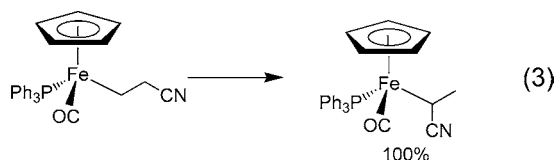


primary metal–alkyl bond is stronger than a secondary metal–alkyl bond.¹²

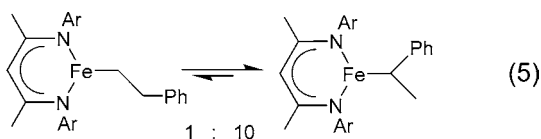
There have been a number of reports, however, where this thermodynamic selectivity can be reversed. Reger also reported that heating the β-cyanoethyl derivative of the iron complex in eq 1 to 95 °C led to the conversion to the branched α-cyanoethyl complex (eq 3).¹³ Likewise, the β-cyanoethyl derivative of the palladium complex in eq 2 rearranges quantitatively to the α-cyanoethyl isomer at 120 °C (eq 4). This change in selectivity for the branched isomer was attributed to the electronic effect of the cyano group on the carbon attached to the metal overcoming the steric effects disfavoring formation of a branched isomer. Harvey has reported, however, that the preference for primary over secondary alkyl derivatives is also primarily an electronic effect, as a result of the fact that primary carbanions are favored over secondary carbanions.¹⁴

Received: January 28, 2013

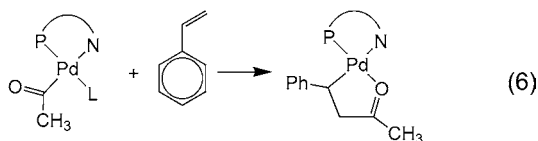
Published: April 23, 2013



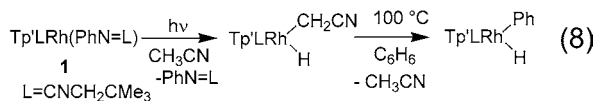
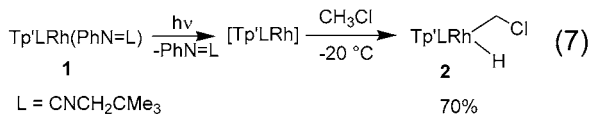
Another example of where the linear/branched product distribution is reversed is oftentimes seen in styrene insertion reactions. For example, Holland reported that insertion of styrene into an iron-nacnac hydride initially gave the linear β -phenethyl product that rearranged to give the thermodynamically preferred α -phenethyl isomer (eq 5).¹⁵ Similarly,



Consiglio reported that insertion of styrene into a palladium-acyl bond led to the branched insertion product rather than the linear insertion product (eq 6).¹⁶ Related observations have been made for other styrene insertions to give branched isomers.^{17,18}



We have been interested in determining quantitatively the effect of substituents on α -substituted alkyl groups during C–H activation reactions of substituted aliphatic hydrocarbons using the [Tp'Rh(CNneopentyl)] fragment, for which extensive thermodynamic data are available for the parent hydrocarbon activations.¹⁹ We have discovered that 1-chloroalkanes show strong selectivity for the activation of a methyl group at the remote end of the chain, and that chloromethane undergoes C–H but not C–Cl oxidative addition (eq 7).²⁰ The product,



Tp'Rh(CNneopentyl)(CH₂Cl)H is reluctant to undergo reductive elimination, which was attributed to the electron withdrawing nature of the α -substituent. Studies were also done on a series of alkyl nitriles, where it was also found that α -cyano substitution gave products that would only undergo reductive elimination at elevated temperatures (eq 8).²¹ This effect was attributed to a strengthening of the metal–carbon bond due to substitution by the electron-withdrawing cyano group.

We also hypothesized that these α -substituent effects, as well as in related α -methyl and methallyl derivatives, led to a correlation of Rh–C bond strengths that was distinct from the correlation seen with unsubstituted hydrocarbons.²² Figure 1

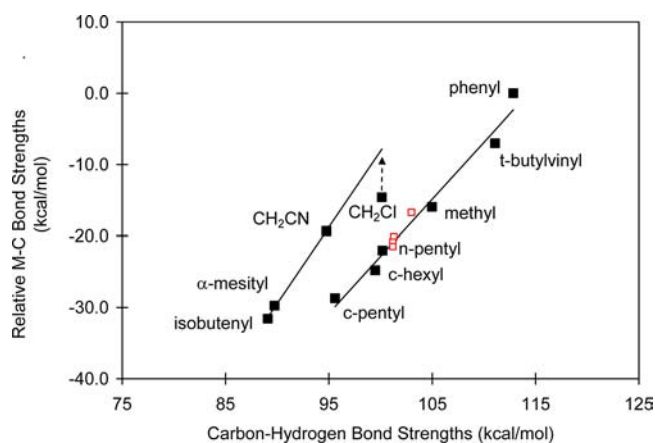


Figure 1. Comparison of rhodium–carbon and hydrogen–carbon bond strengths. The slopes of the upper and lower lines are 2.13 and 1.59, respectively. The data shown in four open red squares are for the primary C–H bond in propionitrile, butyronitrile, valerionitrile, and capronitrile, top to bottom, using DFT calculated C–H bond strengths for these four substrates, but experimental bond strengths for all other C–H bond strengths. Reprinted with permission from ref 22. Copyright 2009 American Chemical Society.

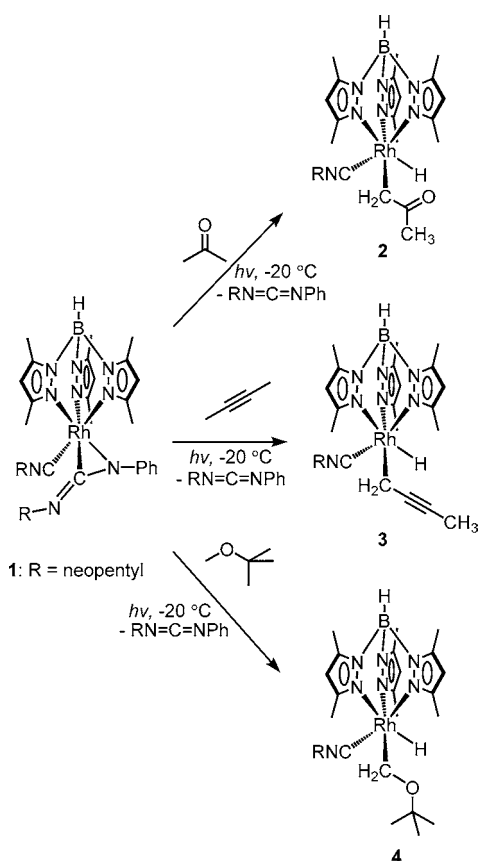
shows the proposed correlations for the two classes of substrates. The lower line contains only sp^3 and sp^2 hydrocarbons. The upper line includes only substituted methyl derivatives of the type Tp'Rh(CNneopentyl)(CH₂X)H. Only three data points were used to formulate this second correlation, and it was deemed necessary to collect additional data to support the hypothesis that these substituted derivatives followed a separate trend. In this contribution, additional data are obtained for the compounds where X = CH₂C(=O)CH₃, CH₂C≡CCH₃, CH₂O-*t*-Bu, CH₂CF₃, CH₂F, and CHF₂. These data are then combined with recently obtained data for terminal alkyne sp C–H activation²³ and pentafluoroarene activation²⁴ to provide a unified picture of the factors that control metal–carbon bond strengths. Some surprises were uncovered.

RESULTS

Synthesis and Characterization of Tp'Rh-(CNneopentyl)(CH₂X)H. Irradiation of Tp'Rh-(CNneopentyl)(PhNCNneopentyl) (1) has proven to be an efficient way to form the coordinatively unsaturated fragment [Tp'Rh(CNneopentyl)] which then reacts with most hydrocarbons to give clean C–H oxidative addition products.²⁵ Kinetic products are obtained, and the observed stabilities of the products toward reductive elimination at room temperature range from minutes (cyclohexane) to hours (methane) to months (benzene).¹⁹ As mentioned above, only a few substrates of the type CH₃X have been examined where X represents a functional group. Scheme 1 shows three additional substrates that have been examined.

Photolysis of 1 in neat acetone resulted in a color change of the solution from bright yellow to pale yellow after only 3 min at -20 °C. ¹H NMR spectroscopic analysis of the product shows clean formation of Tp'Rh(CNneopentyl)(CH₂C(=O)CH₃)H (2) with a hydride resonance at δ -14.778 (d, J_{Rh-H}

Scheme 1. Products from the Photolysis of 1 in Various Substrates



= 19.8 Hz). This small Rh–H coupling constant is typical in α -substituted alkyl hydride complexes (cf. $J = 20$ Hz for $\text{Tp}^*\text{Rh}(\text{CNneopentyl})(\text{CH}_2\text{CN})\text{H}$,²¹ vs $J = 24\text{--}25$ Hz for unsubstituted alkyl and aryl hydride species^{19a}). The diastereotopic methylene resonances of $\text{RhCH}_2\text{C}(=\text{O})\text{CH}_3$ were shifted downfield relative to free acetone and appear at δ 2.871 and 2.993. Similarly, the resonance for the ketone methyl peak was shifted downfield to δ 2.469. Treatment of 2 with CCl_4 gave $\text{Tp}^*\text{Rh}(\text{CNneopentyl})(\text{CH}_2\text{C}(=\text{O})\text{CH}_3)\text{Cl}$ (2-Cl), which was fully characterized by NMR spectroscopy, elemental analysis, and X-ray structure determination (Figure 2). The structure shows an octahedral geometry with a Rh1–C7 distance of 2.109 (3) Å, typical for a Rh–C(sp^3) bond (cf. $d(\text{Rh}–\text{C}) = 2.105$ (4) Å in $\text{Tp}^*\text{Rh}(\text{CNneopentyl})(n\text{-pentyl})\text{Cl}$ ^{19a}).

Photolysis of 1 in 2-butyne at -20 °C led to the rapid formation of $\text{Tp}^*\text{Rh}(\text{CNneopentyl})(\text{CH}_2\text{C}\equiv\text{CCH}_3)\text{H}$ (3) with a hydride resonance at δ -14.567 (d, $J_{\text{Rh}–\text{H}} = 21.9$ Hz) in the ^1H NMR spectrum. In contrast to the activation of acetone, decomposition was observed if the irradiation was continued longer than 3 minutes or at a temperature above -20 °C. In addition, no evidence of an η^2 -coordinated intermediate was observed either during irradiation or upon heating of 3 in benzene (vide infra), which suggests C–H activation has a lower barrier than coordination to the triple bond and that the C–H activation product is thermodynamically more stable than the π -complex.

Photolysis of 1 in 2-methoxy-2-methylpropane required a longer irradiation time for completion (30 min) and produced only one product, $\text{Tp}^*\text{Rh}(\text{CNneopentyl})(\text{CH}_2\text{O}-t\text{-Bu})\text{H}$ (4). The ^1H

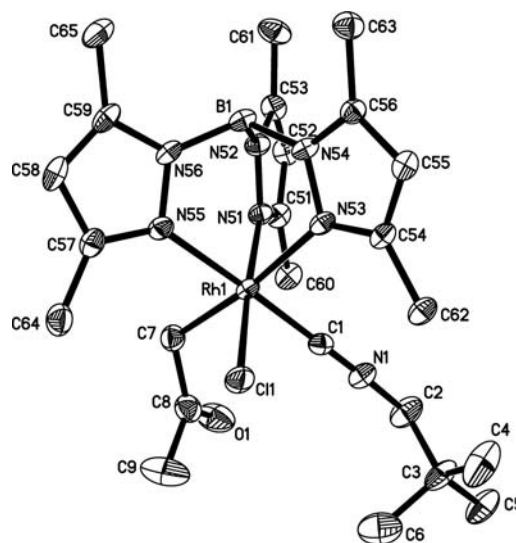


Figure 2. Thermal ellipsoid drawing of $\text{Tp}^*\text{Rh}(\text{CNneopentyl})(\text{CH}_2\text{C}(=\text{O})\text{CH}_3)\text{Cl}$ (2-Cl). Hydrogen atoms have been omitted for clarity. Ellipsoids are shown at the 50% level.

NMR spectrum of 4 displays a hydride doublet at δ -14.403 ($J_{\text{Rh}–\text{H}} = 25.2$ Hz) and a methylene doublet at δ 4.888 ($J_{\text{Rh}–\text{H}} = 16.1$ Hz). The bulky *tert*-butyl group and proximity of the methyl to the electron-rich oxygen atom ensures the exclusive C–H activation at the methyl group. Treatment of 4 with CCl_4 produces $\text{Tp}^*\text{Rh}(\text{CNneopentyl})(\text{CH}_2\text{O}-t\text{-Bu})\text{Cl}$ (4-Cl), which was fully characterized by NMR spectroscopy, elemental analysis, and X-ray structure determination (Figure 3). The

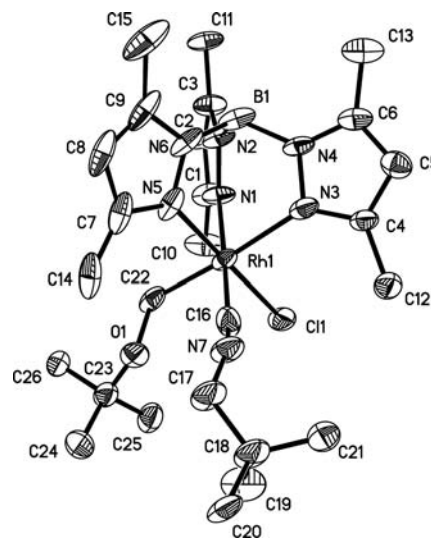


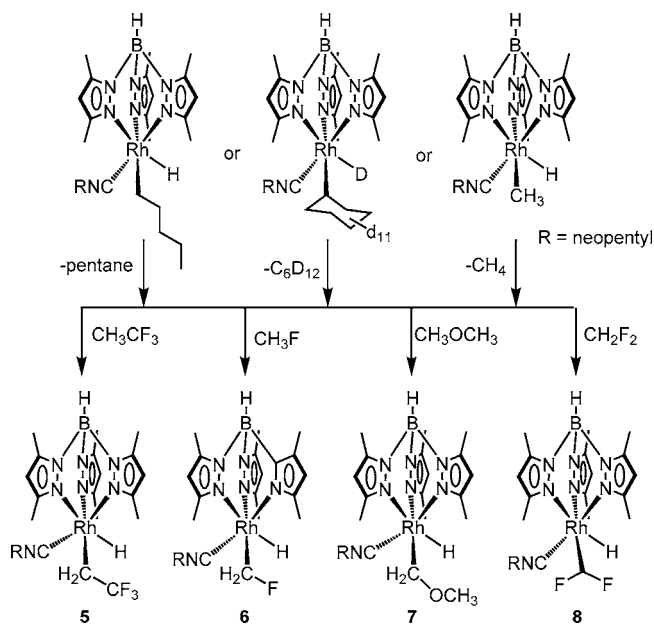
Figure 3. Thermal ellipsoid drawing of $\text{Tp}^*\text{Rh}(\text{CNneopentyl})(\text{CH}_2\text{O}-t\text{-Bu})\text{Cl}$ (4-Cl). Hydrogen atoms have been omitted for clarity. Ellipsoids are shown at the 50% probability level.

structure shows an octahedral geometry with a Rh1–C22 distance of 2.042 (7) Å, somewhat short for a Rh–C(sp^3) bond and more similar to a Rh–C(sp^2) distance (cf. $d_{\text{Rh}–\text{C}} = 2.021$ (6) Å in $\text{Tp}^*\text{Rh}(\text{CNneopentyl})(\text{CH}=\text{CHCMe}_3)\text{Cl}$,^{19b} 2.063 (5) Å in $\text{Tp}^*\text{Rh}(\text{CNneopentyl})(\text{C}_6\text{F}_5)\text{Cl}$,²⁴ and 2.050 (9) in $\text{Tp}^*\text{Rh}(\text{CNneopentyl})(c\text{-propyl})\text{Cl}$.²⁶

Photolysis of 1 in/with fluoroalkanes showed mainly decomposition products. Therefore $\text{Tp}^*\text{Rh}(\text{CNneopentyl})(n\text{-}$

pentyl)H, $\text{Tp}'\text{Rh}(\text{CNneopentyl})(c\text{-C}_6\text{D}_{11})\text{D}$, or $\text{Tp}'\text{Rh}(\text{CNneopentyl})(\text{CH}_3)\text{H}$ were prepared in situ by irradiation of **1** in neat *n*-pentane or cyclohexane-*d*₁₂ or by the reaction of $\text{Tp}'\text{Rh}(\text{CNneopentyl})(\text{CH}_3)\text{Cl}$ with Cp_2ZrH_2 .²⁶ The labile complexes $\text{Tp}'\text{Rh}(\text{CNneopentyl})(\text{R})\text{H}$ (*R* = *n*-pentyl, *c*- C_6D_{11} or CH_3) serve as thermal precursors to the reactive intermediate, $[\text{Tp}'\text{Rh}(\text{CNneopentyl})]$, which then inserts into the C–H bonds of fluoroalkanes (Scheme 2). The mild exchange reactions usually take overnight to several days to go to completion.

Scheme 2. Products from Exchange Reactions with Substrates



Exchange of $\text{Tp}'\text{Rh}(\text{CNneopentyl})(\text{CH}_3)\text{H}$ with CH_3CF_3 led to the clean formation of $\text{Tp}'\text{Rh}(\text{CNneopentyl})(\text{CH}_2\text{CF}_3)\text{H}$ (**5**). **5** was also prepared via reaction with $\text{Tp}'\text{Rh}(\text{CNneopentyl})(n\text{-pentyl})\text{H}$ under a pressure of CH_3CF_3 , but was accompanied by trace amounts of *o*-, *m*-, and *p*-carbodiimide activation products (<5%).^{20b,25} No C–F activation product was detected by NMR spectroscopy. The hydride resonance for **5** appeared as a doublet at $\delta -14.344$ ($J_{\text{Rh-H}} = 21.3$ Hz). The hydride doublet also indicates the absence of coupling between the hydride and any fluorine(s). The ^{19}F NMR spectrum shows a triplet due to coupling with the two neighboring methylene hydrogen atoms. Due to the presence of many couplings, ^1H NMR analysis of the methylene resonance was ambiguous, but a quintet was seen in the $^{13}\text{C}\{^1\text{H}\}$ NMR spectrum at $\delta 8.31$ ($J_{\text{Rh-C}} = J_{\text{F-C}} = 26.9$ Hz). Moreover, an HSQC spectrum indicates that the hydrogen resonances associated with this methylene group were obscured by the *pz*- CH_3 resonances ($\delta 2.134\text{--}2.146$) in the ^1H NMR spectrum (see Supporting Information [SI]).

$\text{Tp}'\text{Rh}(\text{CNneopentyl})(\text{CH}_2\text{F})\text{H}$ (**6**) was prepared via exchange reaction of $\text{Tp}'\text{Rh}(\text{CNneopentyl})(\text{CH}_3)\text{H}$ under a pressure of CH_3F in C_6D_{12} . However, the reaction is quite slow and the yield was only 23% after two weeks. The exchange with more labile $\text{Tp}'\text{Rh}(\text{CNneopentyl})(n\text{-pentyl})\text{H}$ led to a higher conversion, 50% after 5 days. Small amounts of carbodiimide activation products were seen (~10%). The hydride resonance for **6** appeared as a doublet of doublets at $\delta -14.221$ ($J_{\text{Rh-H}} =$

24.7 Hz, $J_{\text{F-H}} = 8.6$ Hz). The fluorine resonance for **6** was observed in the ^{19}F NMR spectrum as a triplet of doublets of doublets with one Rh–F and two H–F couplings. The triplet H–F coupling was due to the two methylene hydrogen atoms, with the other H–F coupling being due to the hydride ($J_{\text{H-F}} = 8.6$ Hz).

An unexpected hydride resonance at $\delta -14.14$ with $J_{\text{Rh-H}} = 25.2$ Hz was observed in both of the above reactions with yields of 28% and 36%, respectively (Figure 4). The ^{19}F NMR

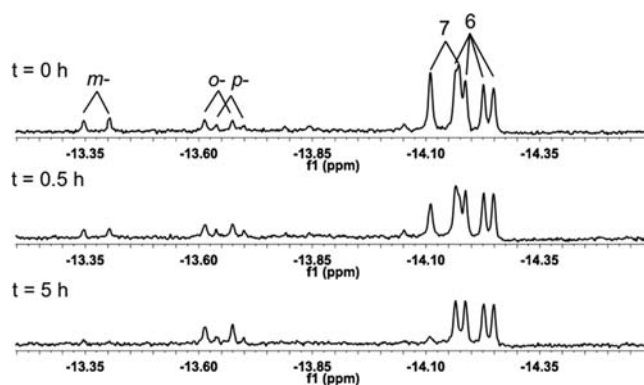


Figure 4. ^1H NMR of hydride region for reductive elimination of a mixture of $\text{Tp}'\text{Rh}(\text{CNneopentyl})(\text{CH}_2\text{F})\text{H}$ (**6**) and $\text{Tp}'\text{Rh}(\text{CNR})(\text{CH}_2\text{OCH}_3)\text{H}$ (**7**) in C_6D_6 at 66.9 °C. Small quantities of *o*-, *m*-, and *p*-carbodiimide activation products can also be identified.

spectrum shows no corresponding fluorine resonance for this byproduct. This hydrido compound was found to produce $\text{Tp}'\text{Rh}(\text{CNneopentyl})(\text{C}_6\text{D}_5)\text{D}$ by reductive elimination in C_6D_6 cleanly. The half-life of 2.0 h at 66.9 °C suggested that it was generated from activation of an impurity in the CH_3F . These properties of the unknown product are similar to those of $\text{Tp}'\text{Rh}(\text{CNR})(\text{CH}_2\text{O-}t\text{-Bu})\text{H}$, in which the hydride resonance appeared at a similar chemical shift ($\delta -14.403$) with the same coupling constant. Further examination of the gas used in the experiment (^1H NMR and GC–MS) allowed the impurity to be identified as dimethyl ether, present at ~16% of the commercial CH_3F sample. Therefore this hydride product was assigned as $\text{Tp}'\text{Rh}(\text{CNR})(\text{CH}_2\text{OCH}_3)\text{H}$ (**7**) from activation of dimethyl ether.

Irradiation of $\text{Tp}'\text{Rh}(\text{CNneopentyl})(\text{carbodiimide})$ in C_6D_{12} followed by addition of CH_2F_2 led to formation of a mixture of $\text{Tp}'\text{Rh}(\text{CNneopentyl})(\text{CHF}_2)\text{H}$ (**8**) and the products of carbodiimide activation (31:69). The hydride resonance appeared at $\delta -14.095$ as a doublet of doublets, suggesting coupling with only one of the two diastereotopic fluorine atoms. Two distinct fluorine resonances were observed at $\delta -11.480$ and $\delta -17.238$ with different coupling patterns, the former showing the same fluorine–hydride coupling constant as that for the hydride resonance in the ^1H NMR spectrum (11.7 Hz). The hydrogen of the difluoromethyl group could not be readily identified, as many couplings were present.

An attempt to activate the C–H bond of CF_3H under similar conditions as those employed for the above studies failed to show evidence for oxidative addition. Perhaps the bulk of the three fluorines prevents formation of the alkane σ -complex that precedes C–H activation.^{9,27}

Reductive Elimination of $\text{Tp}'\text{Rh}(\text{CNneopentyl})(\text{R})\text{H}$. The rates for reductive elimination of complexes **2–7** were determined by monitoring the first order disappearance of the

Table 1. Rates of Reductive Elimination^a of RH from Tp'Rh(CNneopentyl)(R)H in C₆D₆

R	T (°C)	k _{re} (RH), s ⁻¹	τ _{1/2}	ΔG _{re} ^{‡g} kcal·mol ⁻¹
C ₆ H ₅ ^b	66.9	3.78 × 10 ⁻⁷	20.8 d	29.98 (5)
CH ₂ C(=O)CH ₃ , 2	66.9	1.11 (2) × 10 ⁻⁵	17.3 h	27.71 (1)
CH ₂ C≡CCH ₃ , 3	66.9	3.26 (4) × 10 ⁻⁵	5.9 h	26.98 (1)
CH ₂ O- <i>t</i> -Bu, 4	66.9	3.21 (7) × 10 ⁻⁴	0.6 h	25.43 (1)
CH ₂ CF ₃ , 5	66.9	8.31 (22) × 10 ⁻⁶	23.2 h	27.90 (2)
CH ₂ F, 6	66.9	3.54 (12) × 10 ⁻⁶	54.4 h	28.48 (2)
CH ₂ OCH ₃ , 7	66.9	9.7 (11) × 10 ⁻⁵	2.0 h	26.24 (8)
CHF ₂ , 8	100.0	1.28 (4) × 10 ⁻⁵	15.0 h	30.36 (1)
CH ₂ Cl ^c	80	~4 × 10 ⁻⁵	~4.8 h	~27.9
CH ₂ CN ^d	100	2.62(7) × 10 ⁻⁶	73.2 h	31.36 (2)
CH ₃ ^e	23	3.41(13) × 10 ⁻⁵	5.6 h	23.52 (3)
C ₆ F ₅ ^f	138.5	2.46(4) × 10 ⁻⁷	32.5 d	36.81 (1)

^aErrors are reported as standard deviations. ^bRate for reductive elimination was calculated from Eyring plot data in ref 28, ΔG_{re}[‡] = 37.8 - T × 23 = 29.98 kcal mol⁻¹ at 340 K. ^cData for CH₂Cl from ref 20b. ^dData for CH₂CN from ref 21. ^eData for CH₃ from ref 19a. ^fData for C₆F₅ from ref 24. ^gError in ΔG_{re}[‡] calculated using σ_G = (RT/k_{re})σ_k.

hydride resonance in C₆D₆ at 66.9 °C by ¹H NMR spectroscopy (see SI, Tables S1–S13). Generally, reductive eliminations of substituted methanes CH₃X from 2–7 were much slower than the elimination of methane from Tp'Rh-(CNneopentyl)(CH₃)H at room temperature (τ_{1/2} ≈ 5 h). The reductive elimination experiment with 8 was performed at 100.0 °C because no appreciable decrease of the corresponding hydride resonance was detected at 66.9 °C after one week. The corresponding activation barriers for reductive elimination in 2–8 are ~2–7 kcal·mol⁻¹ higher than that in Tp'Rh-(CNneopentyl)(CH₃)H. The rate of CH₂F₂ reductive elimination for 8 is comparable to that for Tp'Rh(CNneopentyl)-(C₆H₅)H, which indicates that the difluoro-substitution greatly stabilizes the compound vs Tp'Rh(CNneopentyl)(CH₃)H.

Competitive Selectivity Experiments. The relative selectivity of the fragment [Tp'Rh(CNneopentyl)] for C–H activation of the various substrates was determined by photolysis of 1 in a mixture of two substrates. The ratio of the two substrates was measured by ¹H NMR analysis before irradiation. The competition experiments were carried out with only 5 min of photolysis at low temperature so that the product ratio represented the kinetic products of the reaction. The product distribution was determined on the basis of the relative areas of the corresponding hydride resonances by ¹H NMR spectroscopy in deuterated solvent (C₆D₆ or C₆D₁₂). The relative competitive rates k₂/k₁ reported in Table 2 were calculated on a per-molecule basis using eq 9, where I₂/I₁ is the integration area of the hydride resonances and n₁/n₂ is the mole ratio of two substrates (subscript 2 refers to benzene and subscript 1 represents the other competing substrate). The differences in free energies of activation ΔΔG_{oa}[‡] can be calculated using eq 10. The results of competition between 2–8 and benzene are included in Table 2 as well as previous results with methane and pentafluorobenzene.

$$\frac{k_2}{k_1} = \left(\frac{I_2}{I_1}\right) \left(\frac{n_1}{n_2}\right) \quad (9)$$

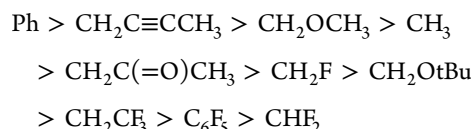
$$\Delta\Delta G_{oa}^{\ddagger} = RT \ln(k_2/k_1) \quad (10)$$

DISCUSSION

As shown in Schemes 1 and 2, both photochemical and thermal methods can be used to generate the fragment [Tp'Rh-

(CNneopentyl)], which underwent activation of only one type of C–H bond in each substrate. As shown in Table 1, substituted products 2–8 underwent reductive elimination much more slowly (τ_{1/2} = 0.6 h to 37 d at 66.9 °C) than the unsubstituted methyl hydride complex (τ_{1/2} = 5.6 h at 23 °C). These results generally indicate that α-substitution at carbon with an electron withdrawing group increases the 'stability' of the alkyl hydride species, or more properly, decreases the lability of the alkyl hydride.²⁹ Among 2–8, elimination of *tert*-butyl methyl ether from 4 is the fastest (τ_{1/2} = 0.6 h), followed by the less bulky dimethyl analogue 7 (τ_{1/2} = 2.0 h). An unsaturated substituent improves the stability to some extent as shown in complexes 2 and 3 (τ_{1/2} = 17.3 and 5.9 h). Fluoro substitution had a stronger effect on the stability in the order CH₂CF₃ < CH₂F < CHF₂, in which substitution at the β-site increases the stability to a lesser extent than substitution at the α-site, and di-fluorination is far superior to mono-fluorination. These observations are in agreement with earlier studies of alkylnitriles and alkyl chlorides, where α-substitution had the most dramatic effect on stability.^{20,21} The difference between fluorination and chlorination on stabilization is minimal – the barrier for elimination of CH₂F vs CH₂Cl is only ~0.6 kcal mol⁻¹ higher for the former. A cyano substituent dramatically stabilizes the corresponding cyanomethyl hydride complex compared to an α-keto (2) or α-alkynyl (3) group probably due to its higher electron-withdrawing capability.

The kinetic selectivity of the coordinatively unsaturated intermediate [Tp'Rh(CNneopentyl)] toward the substrates R–H discussed above follows the order:



Generally, activation of many of the substituted methanes is kinetically less preferable than activation of methane. This could be attributed to the steric effect of α-substitution as the order of selectivity follows approximately the size of the substituent attached to the α-carbon. Steric effects may interfere with the formation of an alkane σ-complex prior to C–H oxidative cleavage. It is interesting to compare activation of methyl *tert*-butyl ether vs dimethyl ether, in which the free energy of activation (ΔG_{oa}[‡]) of the former is ~0.4 kcal·mol⁻¹ higher than that of the latter. This kinetic difference can be

attributed to statistical factors favoring the activation of dimethyl ether ($RT \ln 2 = 0.4 \text{ kcal mol}^{-1}$).

With the data for reductive elimination and kinetic selectivity shown in Tables 1 and 2, the relative free energies for

Table 2. Kinetic Selectivity Data Determined from Competition Experiments^a

entry	substrates	T (°C)	k_2/k_1^b	$\Delta\Delta G_{\text{oa}}^{\ddagger c}$ (kcal mol ⁻¹)
1	benzene: acetone	8	3.71 (19)	0.73 (3)
2	benzene: 2-butyne	10	2.17 (11)	0.44 (3)
3	benzene: MeOtBu	8	4.53 (23)	0.84 (3)
4	benzene: CH ₃ OCH ₃	10	2.33 (12)	0.48 (3)
5	benzene: CH ₃ CF ₃	10	18.2 (9)	1.63 (3)
6	benzene: CH ₃ F	10	4.24 (21)	0.81 (3)
7	benzene: CH ₂ F ₂	10	62.9 (31)	2.33 (3)
8	benzene: methane ^d	22	3.31 (17)	0.70 (3)
9	benzene: C ₆ F ₅ ^e	10	30.2 (15)	1.92 (3)

^aEach sample was irradiated for 5 min. ^bErrors in rate ratio estimated at 5% for proton NMR integration, giving $\sigma_G = (RT/\text{ratio})\sigma_{\text{ratio}} = 0.05RT \approx 0.03 \text{ kcal mol}^{-1}$ (see Figures S-21 to S-26 in SI). ^cA positive value denotes that benzene is kinetically favored. ^dData are calculated from methane vs pentane at room temperature and pentane vs benzene at $-15 \text{ }^\circ\text{C}$ from ref 22. ^eData are from ref 24.

compounds 2–8 vs Tp’Rh(CNneopentyl)(Ph)H were calculated using eq 11 (a positive ΔG° implies benzene is thermodynamically favored). Since the temperature at which the reductive elimination rates were measured for the various RH substrates varied from 22 to 138 °C, the ΔG^\ddagger for benzene reductive elimination at each temperature was calculated from the known activation parameters for use in eq 11.^{28,30} The relative metal–carbon bond energies compared to $D(\text{Rh–Ph})$ were then calculated on the basis of the experimental values of carbon–hydrogen bond energies $D(\text{R–H})$ using eq 12. Note that the statistics for the entropic contribution to $\Delta\Delta G^\ddagger$ are removed by inclusion of the $RT \ln(6/\#H)$ term where #H is the number of C–H bonds available for oxidative addition (Table 3).

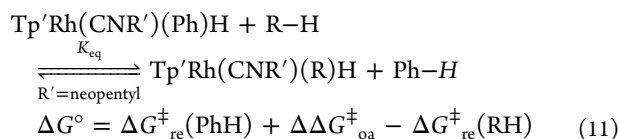


Table 3. Kinetic and Thermodynamic Data for Tp’Rh(CNneopentyl)(R)H^a

RH	no. of H	$\Delta\Delta G_{\text{oa}}^\ddagger$	ΔG°	$D(\text{R–H})^b$	$D_{\text{rel}}(\text{Rh–C})$
benzene	6	0.00	0.00 (5)	112.9	0.0
CH ₃ CF ₃	3	1.63 (3)	3.71 (10)	106.7	–9.5
CH ₂ F ₂	2	2.33 (3)	1.19 (9)	103.2	–10.2
CH ₃ F	3	0.81 (3)	2.31 (10)	101.3	–13.5
CH ₄ ^c	4	0.70 (3)	8.17 (11)	105.0	–15.8
CH ₃ CN ^c	3	1.48 (3)	–0.66 (10)	94.8	–17.0
acetone	6	0.73 (3)	3.00 (9)	96.0	–19.9
dimethyl ether	6	0.48 (3)	4.22 (16)	96.1	–21.0
methyl <i>tert</i> -butyl ether	3	0.84 (3)	5.39 (9)	93.0 ^e	–24.9
2-butyne	6	0.44 (3)	3.44 (9)	90.7	–25.6
C ₆ HF ₅ ^f	1	1.92 (3)	–6.57 (9)	116.5	+11.2

^aAll values are in kcal·mol⁻¹. ^bHydrocarbon C–H bond strengths are from Luo, Y.-R. *Comprehensive Handbook of Chemical Bond Energies*; CRC Press: Boca Raton, FL, 2007. ^cData from ref 22. ^dData from ref 21. ^eThe bond strength for methyl *tert*-butyl ether is not experimentally known; therefore, the value for methyl ethyl ether was used instead. ^fData from ref 24.

$$\begin{aligned} D_{\text{rel}}(\text{Rh–C}) &= [\Delta H(\text{Rh–R}) - \Delta H(\text{Rh–Ph})] \\ &= [D(\text{R–H}) - D(\text{Ph–H})] - \Delta G^\circ + \\ &\quad RT \ln(6/\#H) \end{aligned} \quad (12)$$

Note that all of the Rh–C bond strengths for these substituted derivatives are weaker than the Rh–Ph bond (except for perfluorophenyl). Furthermore, when the substituents are compared as Rh–CH₂–X derivatives of the Rh–CH₃ parent complex, it can be seen that fluorine substituents (or CF₃) increase the Rh–C bond strength whereas groups that weaken the Rh–C bond can engage in resonance or have weakly electron withdrawing groups (e.g., –OR).

Plotting of these relative Rh–C bond energies vs C–H bond energies along with previously determined data shows two distinct correlations²² as shown in Figure 5. The lower line (blue squares) connects sp, sp², and sp³ hydrocarbons with no functional groups and has a slope of 1.38 (3). These substrates include terminal alkynes, terminal alkenes, benzene, and alkanes. Siegbahn noted this same trend in DFT calculations of metal–carbon bond strengths for second row transition metal atoms.³¹ The upper line (red triangles) connects substituted methanes. The slope of 1.40 (14) is indistinguishable from that for the unsubstituted hydrocarbons, and is offset vertically by +7.5 kcal mol⁻¹ from the hydrocarbon line. *This offset represents the increase in the metal–carbon bond strength due to the presence of the substituent relative to the M–C bond strength that would be predicted based upon the strength of the C–H bond that was broken. However, the effect of the substituent, and in particular the substituents that are in hyperconjugation with the M–C bond, is to weaken the M–CH₂X bond relative to M–CH₃.* In the case of CH₂F and CF₂H, the M–C bonds are actually stronger than the M–CH₃ bond. CH₂CF₃, with its three β-fluorines, shows a very slight increase in metal–carbon bond strength. This result is consistent with the observation by Reger that (Me₂NCS₂)(PEt₃)Pd(CH₂CH₂CF₃) and (Me₂NCS₂)(PEt₃)Pd[CH(CH₃)(CF₃)] form in a 1:1 equilibrium, whereas (Me₂NCS₂)(PEt₃)Pd(CH₂CH₂CN) isomerizes completely to (Me₂NCS₂)(PEt₃)Pd[CH(CH₃)(CN)],⁶ implying that CF₃ substitution on a methyl group has only a minor effect on the M–C bond strength.

For comparison with the experimental system, DFT calculations were performed on a broad scope of substituted and unsubstituted substrates using the simplified model

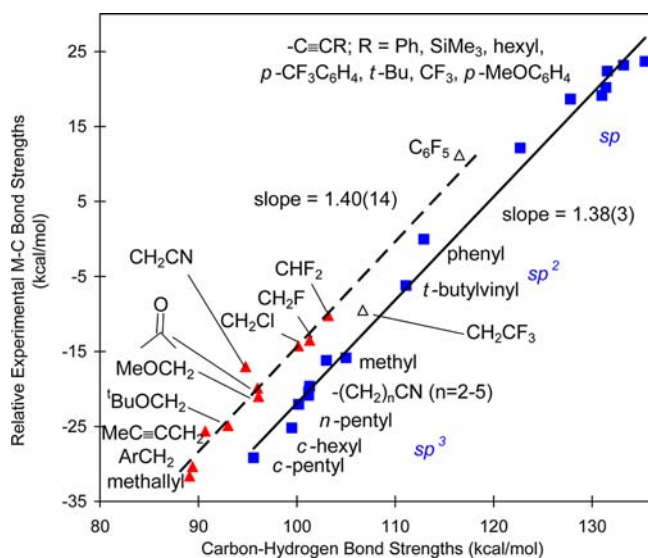


Figure 5. Plot of relative experimental M–C bond strengths vs C–H bond strengths. The solid line is fit to the hydrocarbons and aliphatic nitriles $-(\text{CH}_2)_n\text{-CN}$ ($n = 2-5$) (blue ■, $y = 1.376x - 159.5$), and the dashed line is fit to the $-\text{CH}_2\text{X}$ substrates and $-\text{CHF}_2$ (red ▲, $y = 1.4024x - 154.6$). Also shown are $-\text{C}_6\text{F}_5$ and $-\text{CH}_2\text{CF}_3$ (Δ), which are not included in either fit. Experimental C–H bond strengths were used for all substrates except the alkynes and nitriles (except acetonitrile). Alkyne and nitrile C–H bond strengths were calculated (B3LYP) since experimental values are unavailable or have large errors.²³ The vertical separation of the lines at $D_{\text{C-H}} = 100 \text{ kcal mol}^{-1}$ is $7.5 \text{ kcal mol}^{-1}$.

fragment $[\text{HB}(3,5\text{-dimethylpyrazolyl})_3\text{Rh}(\text{CNMe})]$ (see SI for details). A plot of calculated relative Rh–C bond strengths vs the experimental (or calculated for alkyne) C–H bond strengths within these substrates also shows two distinct linear correlations with slopes of 1.59 and 1.46 for the analogous two sets of compounds (Figure 6). There is generally good agreement with the observed experimental trends in Rh–C bond strengths, but DFT overestimates the range of Rh–C bond strengths by 4–15%.

While the majority of products form Rh– CH_2X bonds that are weaker than the Rh–methyl bond, the bonds are not as weak as one would anticipate by comparing H– CH_2X and H– CH_3 bond energies. The C–H bonds are weak in many of the substrates because the substituent can stabilize the radical after the rupture of C–H bond through resonance. However, the ionic contribution to the M–R bond is more important, as the ionization potential is smaller for a metal than for hydrogen, which indicates the charge distribution (ionicity) dominates the bond strength, as pointed out by Siegbahn,³¹ Harvey,¹⁴ and Clot.³² This could also account for the strengthening of M–R bonds through purely inductive effects as in M– CH_2F and M– CHF_2 (although Siegbahn's calculations of bond strengths with rhodium atoms indicates little effect of fluorine substitution on bond strength³³). Therefore either unsaturated substituents or electronegative functional groups can contribute to strengthening the M–C bond by polarizing electron density from the metal center to the carbon atom, leading to Rh–C bonds that are stronger than expected on the basis of the C–H bond that was broken. The current results also indicate the difluoromethyl hydride complex contains a more ionic Rh–C bond than that in fluoromethyl hydride species. The postulation that direct repulsion from alkyl groups will weaken the resulting M–C

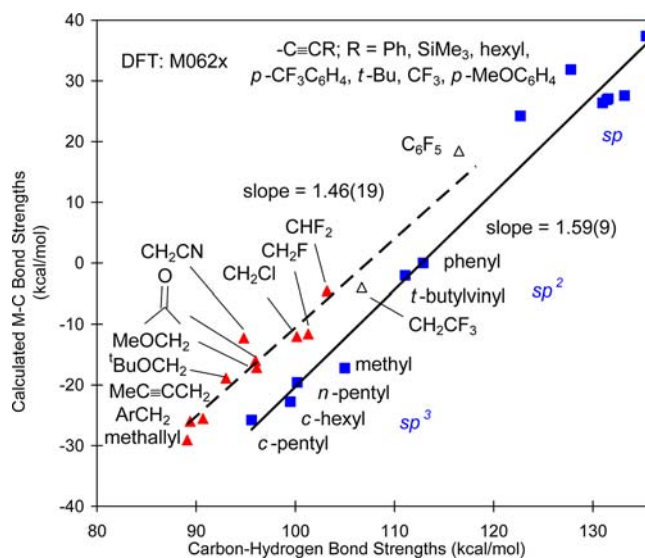


Figure 6. DFT calculated plot of relative M–C bond strengths vs C–H bond strengths for $\text{Tp}'\text{Rh}(\text{CNMe})(\text{R})\text{H}$. The lower line is fit to the hydrocarbons (blue ■, $y = 1.593x - 179.6$), and the upper line is fit to the $-\text{CH}_2\text{X}$ and CHF_2 substrates (red ▲, $y = 1.457x - 156.2$). Data for $\text{C}_6\text{F}_5\text{H}$ and CH_3CF_3 activation is also shown (Δ), but not included in the fits. M06-2X method and basis set 6-31g** for first row atoms and pseudopotentials, additional functions optimized by Stuttgart group for atoms beyond the second row (see ref 23 for details on the choice of method). Experimental C–H bond strengths were used for all substrates except the alkynes. Alkyne C–H bond strengths were calculated (B3LYP) since experimental values are unavailable or have large errors.²³ The vertical separation of the lines at $D_{\text{C-H}} = 100 \text{ kcal mol}^{-1}$ is $9.7 \text{ kcal mol}^{-1}$.

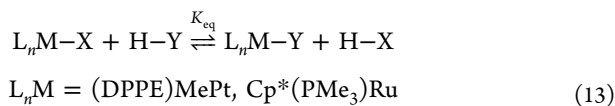
bonds can be excluded or at least have minimal effect here, as bulkier Rh– CHF_2 is still stronger than Rh– CH_2F . The increase in bond strength is therefore associated with an increase in the ionic character of the metal–carbon bonding. Sakaki has reported calculations on $\text{Pd}(\text{PH}_3)_2(\text{CH}_3)\text{H}$ and $\text{Pd}(\text{PH}_3)_2(\text{CH}_2\text{CN})\text{H}$ and their $(\text{H}_2\text{PCH}_2\text{CH}_2\text{PH}_2)$ analogues. He concluded that charge transfer from Pd to the CH_2CN ligand was greater than in the CH_3 ligand, due to the mixing of the $\pi^*(\text{CN})$ and $\sigma^*(\text{C-H})$ orbitals to give a lower energy acceptor orbital in CH_3CN vs the $\sigma^*(\text{C-H})$ in CH_4 .³⁴ In contrast to the present study, however, Sakaki calculated that the Pd– CH_2CN bond was some 11–16 kcal mol^{-1} stronger than the Pd– CH_3 bond.

There are other, more general aspects of this study that are worth mentioning. First, the thermodynamics of a hydrocarbon exchange reaction are controlled by the bonds that are broken and formed. Here, acetonitrile activation is strongly thermodynamically preferred over methane activation (by $\sim 9 \text{ kcal mol}^{-1}$) despite the fact that the product $\text{Tp}'\text{Rh}(\text{CNneopentyl})(\text{CH}_2\text{CN})\text{H}$ has a slightly weaker Rh–C bond (by 1.2 kcal mol^{-1}). One way to think about this is that in an equilibrium between methane and acetonitrile, cleavage of the acetonitrile C–H bond ($94.8 \text{ kcal mol}^{-1}$) means that a methane C–H bond ($105.0 \text{ kcal mol}^{-1}$) has been left intact. It is this difference that gives the large thermodynamic driving force favoring acetonitrile activation.

Another seemingly contradictory point that arises from this study is the observed 'stability' of $\text{Tp}'\text{Rh}(\text{CNneopentyl})(\text{CH}_2\text{CN})\text{H}$ vs $\text{Tp}'\text{Rh}(\text{CNneopentyl})(\text{CH}_3)\text{H}$. The former has a half-life of 3 days at 100°C whereas for the latter it is only 5 h at 25°C . Why should the molecule with the weaker

Rh–C bond appear to be much more ‘stable’ than the molecule with the stronger Rh–C bond? The answer lies in the recognition that heating a molecule to induce reductive elimination represents a measure of the kinetics of that reaction, not the thermodynamics of the elimination. That is, we really mean that $\text{Tp}'\text{Rh}(\text{CNneopentyl})(\text{CH}_2\text{CN})\text{H}$ is *less labile* than $\text{Tp}'\text{Rh}(\text{CNneopentyl})(\text{CH}_3)\text{H}$ when we observe its reluctance to lose acetonitrile. The reason for this can be seen by comparison of the transition states for reductive elimination. In the case of $\text{Tp}'\text{Rh}(\text{CNneopentyl})(\text{CH}_2\text{CN})\text{H}$, a $\sigma\text{-C,H-CH}_3\text{CN}$ complex is formed with a weak C–H bond (95 kcal mol^{-1}) as acetonitrile is lost. In the case of $\text{Tp}'\text{Rh}(\text{CNneopentyl})(\text{CH}_3)\text{H}$, a $\sigma\text{-C,H-CH}_4$ complex is formed with a strong C–H bond ($105 \text{ kcal mol}^{-1}$) as methane is lost. The barrier for methane loss is lower than for acetonitrile because of the greater strength of the C–H bond that is formed in the transition state, lowering its energy.

Several groups have reported related relationships between product stabilities and the difficulty of C–H activation, which was quantitatively expressed by plotting metal–carbon bond energies in the products versus the corresponding known carbon–hydrogen bond strengths in the substrates. The examination by Bryndza and Bercaw in 1987 of the correlation between metal–heteroatom and heteroatom–hydrogen bond energies indicates that the difference between H–X and H–Y BDEs is the same as the difference in M–X and M–Y BDEs (i.e., related by a slope of 1.0).³⁵ This is reasonable only if the equilibrium constants K_{eq} in eq 13 were measured to be approximately unity. The relative bond energies of $L_n\text{M-R}$ (R = alkyl, alkenyl, aryl, alkynyl, etc.) were included and varied over a range of 40 kcal mol^{-1} from R = CH_2Ph to $\text{C}\equiv\text{CR}'$.

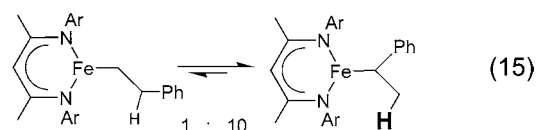
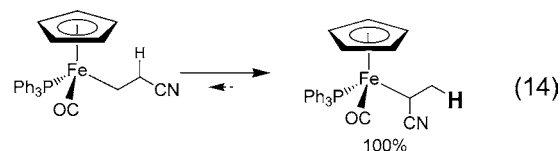


Wolczanski studied a number of $(t\text{-Bu}_3\text{SiO})_2(t\text{-Bu}_3\text{SiNH})\text{-TiR}$ compounds, which displayed a strong correlation of $D(\text{TiR})_{\text{rel}}$ with $D(\text{RH})$ with a slope of 1.1 when the data for R = Bz, Mes, H, and Ph were removed.³⁶ The observation of a slope >1 indicates about a 10% increase in Ti–R bond strengths relative to R–H bond strengths, which implies thermodynamic control of the product distribution. The data for toluene and mesitylene lay above the line and expressed additional stabilization of $\sim 6\text{--}7 \text{ kcal/mol}$, which presumably has its origin due to the similar effects quantified here.

Eisenstein and Perutz have examined the above titanium and $\text{Tp}'\text{Rh}$ systems computationally, where both M–C and C–H bond strengths can be calculated using DFT. They found reasonably good correlations for the substrates examined (all hydrocarbons), with the exception of benzyl and allyl, which lay above the correlation line.³⁷ In studying the activation of polyfluorobenzenes with a variety of metal complexes (Zr–Ni), they found good correlations with slopes in the range 1.9–3.0.³² Landis has also summarized and compared a number of systems where some correlation between M–X and X–H (X includes C) bond strengths has been observed.³⁸

Finally, we return to the issues first raised at the beginning of this manuscript, the control of regioselectivity in olefin insertion reactions. Consider the insertion of an alkene to give a linear or branched hydrocarbon as shown in eq 1 or 2. Is the linear product favored because the primary carbon–metal bond is stronger than the secondary carbon–metal bond? Yes.

Examination of Figure 5 shows that primary carbon–rhodium bonds are stronger than secondary carbon–rhodium bonds. Now consider the insertion of acrylonitrile as shown in eqs 3 and 4. Is the branched product favored over the linear product because the metal–carbon bond is stronger? *No*. In fact, the metal–carbon bond is weaker in the branched product because homolysis leads to a radical that is resonance stabilized, vs a primary radical in the linear product. The same applies to styrene insertion in eq 5. Figure 5 also shows that $\text{Rh-CH}_2\text{CN}$ and $\text{Rh-CH}_2\text{Ph}$ are weaker than Rh-CH_3 . So why are the branched products favored in the nitrile–substituted (and phenyl–substituted) products if the metal–carbon bonds are weaker? The answer is shown in eqs 14 and 15, where the C–H



bond that is also formed/broken is emphasized. In the branched products, a strong primary methyl C–H bond is formed ($\sim 100 \text{ kcal mol}^{-1}$), whereas in the linear product a weak α -cyano or weak benzylic secondary C–H bond is formed ($\sim 88\text{--}92 \text{ kcal mol}^{-1}$). In the substituted derivatives, it is the formation of the (largely ignored) C–H bond that determines the product selectivity, not the metal–carbon bond strength! On this basis, many of the prior statements in the literature (including our own) regarding metal–carbon bond strengths in compounds with α -electron-withdrawing substituents need to be re-evaluated.

CONCLUSIONS

In this work, we have taken kinetic measurements for the reductive elimination of R–H in a series of $\text{H-Rh-CH}_2\text{X}$ complexes and determined the relationship between the relative M–C bond energies and C–H bond energies. The stabilization effect by α -substitution on Rh–methyl has been quantified and shows that the substituents aryl, vinyl, alkynyl, alkoxy, CN, and keto all weaken the $\text{Rh-CH}_2\text{X}$ bond compared to the Rh–methyl bond. While these metal–carbon bonds are weaker than in the Rh–methyl complex, they are not as weak as one would expect on the basis of the relative C–H bond strengths (methane vs $\text{H-CH}_2\text{X}$). Hence, the substituent is having a positive effect on strengthening the metal–carbon bond. Fluorine or chlorine substitution slightly increases the Rh–methyl bond strength, and difluoro substitution strengthens the bond by almost 6 kcal mol^{-1} . The stabilization effect is believed to result from increased polarization of the M–C bond, adding more ionic character.

EXPERIMENTAL SECTION

General Procedures. All operations and routine manipulations were performed under a nitrogen atmosphere, either on a high-vacuum line using modified Schlenk techniques or in a Vacuum Atmospheres Corp. Dri-Lab. Acetone, acetonitrile, carbon tetrachloride, bromoform, methyl *tert*-butyl ether, and 2-butyne were purchased from Aldrich Chemical Co. Fluoromethane, difluoromethane, trifluoromethane and

α,α,α -trifluoroethane were purchased from Matrix Scientific and used straight from lecture bottles. Benzene- d_6 was purchased from Cambridge Isotopes. Prior to use it was distilled under vacuum from a dark purple solution of benzophenone ketyl and stored in an ampule with a Teflon valve. Acetone was distilled under vacuum from a solution dried over potassium carbonate. Carbon tetrachloride was distilled under vacuum from a solution dried over calcium chloride. Methyl *tert*-butyl ether was purchased dry and used straight from bottle with a sure-seal cap. 2-Butyne was distilled under vacuum after drying over molecular sieves. Preparation of Tp'Rh(CNneopentyl)(η^2 -PhN=C=Nneopentyl) (**1**) has been previously reported.²⁵

All photolysis experiments were performed using a 200 W Hg(Xe) arc lamp purchased from Oriol, which was fitted with a water-filled IR filter and a 300 nm low pass filter. Low temperatures were maintained with methanol/N₂ in a Pyrex Dewar. All ¹H and ¹³C NMR spectra were collected on either a Bruker Avance 400 or Avance 500 MHz spectrometer. All HSQC experiments were done on an Avance 500 MHz spectrometer. All chemical shifts were reported in ppm (δ) referenced to the chemical shifts of residual solvent resonances (C₆H₆, δ 7.16 or 128.0). While ¹H chemical shifts are given to 3 decimal places (± 0.4 Hz), these values can vary slightly with concentration and temperature. ¹³C shifts are given to 2 decimal places (± 1 Hz). Elemental analysis was performed by the University of Rochester using a Perkin-Elmer 2400 series II elemental analyzer in CHN mode. All kinetic plots and least-squares error analysis were done using Microsoft Excel.

Preparation of Tp'Rh(CNneopentyl)(CH₂C(=O)CH₃)H (2). A solution of **1** (6 mg, 0.013 mmol) dissolved in 0.4 mL of acetone was placed in an NMR tube sealed with a Teflon cap. This sample was irradiated for 3 min at -20 °C, as the bright yellow solution photobleached to a pale yellow. The solvent was immediately removed *in vacuo* at -20 °C. The resulting pale-yellow residue was dissolved in C₆D₆. ¹H NMR (400 MHz, C₆D₆): δ -14.778 (d, 1 H, ¹J_{Rh-H} = 19.8 Hz, Rh-H), 0.712 (s, 9 H, C(CH₃)₃), 2.142 (s, 3 H, pz-CH₃), 2.169 (s, 3 H, pz-CH₃), 2.268 (s, 3 H, pz-CH₃), 2.317 (s, 3 H, pz-CH₃), 2.469 (s, 3 H, COCH₃), 2.530 (s, 3 H, pz-CH₃), 2.840 (s, 3 H, pz-CH₃), 2.871 (dd, ²J_{Rh-H} = 5.3 Hz, ²J_{H-H} = 3.3 Hz, 1 H, RhCH₂CO), 2.993 (dd, ²J_{Rh-H} = 5.7 Hz, ²J_{H-H} = 3.6 Hz, 1 H, RhCH₂CO), 2.920 (d, ²J_{H-H} = 14.0 Hz, 1 H, NCH₂), 3.131 (d, ²J_{H-H} = 14.0 Hz, 1 H, NCH₂), 5.593 (s, 1 H, pz-H), 5.610 (s, 1 H, pz-H), 5.822 (s, 1 H, pz-H). ¹³C{¹H} NMR (500 MHz, C₆D₆): δ 12.43 (s, 1 C, pz-CH₃), 12.59 (s, 1 C, pz-CH₃), 12.78 (s, 1 C, pz-CH₃), 14.72 (s, 1 C, pz-CH₃), 15.55 (s, 1 C, pz-CH₃), 16.18 (s, 1 C, pz-CH₃), 21.02 (d, ¹J_{Rh-C} = 20.6 Hz, 1 C, RhCH₂CO), 26.70 (s, 3 C, CH₂C(CH₃)₃), 28.73 (s, 1 C, CH₃), 31.49 (s, 1 C, CH₂C(CH₃)₃), 56.72 (s, 1 C, RhCNCH₂), 105.55 (s, 1 C, pz-CH), 106.77 (s, 1 C, pz-CH), 106.78 (s, 1 C, pz-CH), 143.26 (s, 1 C, pz-C), 143.68 (s, 1 C, pz-C), 144.00 (s, 1 C, pz-C), 149.26 (s, 1 C, pz-C), 150.40 (s, 1 C, pz-C), 150.64 (s, 1 C, pz-C), 216.68 (s, 1 C, CO).

Preparation of Tp'Rh(CNneopentyl)(CH₂C \equiv CCH₃)H (3). A solution of **1** (6 mg, 0.013 mmol) dissolved in 0.4 mL of 2-butyne was placed in an NMR tube sealed with a Teflon cap. This sample was irradiated for 3 min at -20 °C or until bright yellow solution photobleached to pale yellow. The solvent was immediately removed *in vacuo* at -20 °C. The resulting yellow residue was dissolved in C₆D₆. ¹H NMR (400 MHz, C₆D₆): δ -14.567 (d, 1 H, ¹J_{Rh-H} = 21.9 Hz, Rh-H), 0.783 (s, 9 H, C(CH₃)₃), 1.742 (br, 3H, C \equiv CCH₃), 2.181 (s, 3 H, pz-CH₃), 2.196 (s, 3 H, pz-CH₃), 2.283 (s, 3 H, pz-CH₃), 2.349 (s, 3 H, pz-CH₃), 2.502 (m, 1 H, RhCH₂C \equiv C), 2.584 (s, 3 H, pz-CH₃), 2.657 (m, 1 H, RhCH₂C \equiv C), 2.699 (s, 3 H, pz-CH₃), 2.796 (s, 2 H NCH₂), 5.600 (s, 1 H, pz-H), 5.626 (s, 1 H, pz-H), 5.785 (s, 1 H, pz-H). ¹³C{¹H} NMR (500 MHz, C₆D₆): δ -11.88 (d, ¹J_{Rh-C} = 22.4 Hz, 1 C, RhCH₂), 5.20 (s, 1 C, C \equiv CCH₃), 12.57 (s, 1 C, pz-CH₃), 12.59 (s, 1 C, pz-CH₃), 12.78 (s, 1 C, pz-CH₃), 14.42 (s, 1 C, pz-CH₃), 15.35 (s, 1 C, pz-CH₃), 15.70 (s, 1 C, pz-CH₃), 26.58 (s, 3 C, CH₂C(CH₃)₃), 32.15 (s, 1 C, CH₂C(CH₃)₃), 58.58 (s, 1 C, RhCNCH₂), 70.62 (s, 1 C, RhCH₂C \equiv C), 93.13 (s, 1 C, RhCH₂C \equiv C), 105.380 (s, 1 C, pz-H), 106.29 (s, 1 C, pz-H), 106.41 (s, 1 C, pz-H), 143.09 (s, 1 C, pz-C), 143.14 (s, 1 C, pz-C), 143.39 (s, 1 C, pz-C), 148.98 (s, 1 C, pz-C), 149.67 (s, 1 C, pz-C), 150.93 (s, 1 C, pz-C).

Preparation of Tp'Rh(CNneopentyl)(CH₂O-*t*-Bu)H (4). A solution of **1** (9 mg, 0.013 mmol) dissolved in 0.5 mL of methyl *tert*-butyl ether was placed in an NMR tube sealed with a Teflon cap. This sample was irradiated for 30 min at -20 °C. The solvent was immediately removed *in vacuo* at room temperature. The resulting yellow residue was dissolved in C₆D₆. ¹H NMR (400 MHz, C₆D₆): δ -14.403 (d, ¹J_{Rh-H} = 25.2 Hz, 1 H, Rh-H), 0.741 (s, 9 H, C(CH₃)₃), 1.340 (s, 9 H, O-C(CH₃)₃), 2.211 (s, 3 H, pz-CH₃), 2.232 (s, 3 H, pz-CH₃), 2.318 (s, 3 H, pz-CH₃), 2.400 (s, 3 H, pz-CH₃), 2.664 (s, 3 H, pz-CH₃), 2.721 (s, 3 H, pz-CH₃), 2.788 (s, 2 H, NCH₂), 4.888 (d, ²J_{Rh-H} = 16.1 Hz, 2 H, RhCH₂O), 5.645 (s, 1 H, pz-H), 5.656 (s, 1 H, pz-H), 5.868 (s, 1 H, pz-H). ¹³C NMR (500 MHz, C₆D₆): δ 12.68 (s, 2 C, pz-CH₃), 12.91 (s, 1 C, pz-CH₃), 14.56 (s, 1 C, pz-CH₃), 15.31 (s, 1 C, pz-CH₃), 15.64 (s, 1 C, pz-CH₃), 26.85 (s, 3 C, OC(CH₃)₃), 28.17 (s, 3 C, CH₂C(CH₃)₃), 31.74 (s, 1 C, CH₂C(CH₃)₃), 53.88 (d, ¹J_{Rh-C} = 26.1 Hz, 1 C, RhCH₂O), 55.97 (s, 1 C, RhCNCH₂), 72.88 (s, 1 C, OC(CH₃)₃), 102.26 (s, 1 C, pz-H), 106.25 (s, 1 C, pz-H), 106.37 (s, 1 C, pz-H), 142.96 (s, 1 C, pz-C), 143.22 (s, 1 C, pz-C), 143.56 (s, 1 C, pz-C), 148.83 (s, 1 C, pz-C), 149.85 (s, 1 C, pz-C), 150.61 (s, 1 C, pz-C).

Preparation of Tp'Rh(CNneopentyl)(CH₂CF₃)H (5). *Method A.* To a yellow solution of 10 mg (0.018 mmol) of Tp'Rh(CNneopentyl)(CH₃)Cl in 1 mL of THF was added 4 mg (0.018 mmol) of Cp₂ZrH₂. The suspension was stirred for 30 min and changed from light yellow to white. The slurry was transferred to a high pressure NMR tube after filtration through a glass wool plug. Removal of the volatiles gave a white residue to which was added 0.5 mL C₆D₁₂ to give white cloudy suspension after sonication. The tube was then pressurized with 30 psi of CH₃CF₃ and shaken carefully at room temperature. ¹H NMR spectroscopic analysis shows 51% conversion to **5** after standing overnight at room temperature. Complete conversion was achieved after 2 days. The slurry was then filtered and a clear colorless solution was obtained, giving a white crystalline solid after evaporation. The formation of **5** was confirmed by elemental analysis and NMR analysis in C₆D₆ (see below). Remarkably, **5** did not react with excess CCl₄. It also has a surprising resistance to air, lasting over one week.

Method B. Eight mg (mmol) of **1** was partially dissolved in 0.5 mL pentane and led to a pale yellow clear solution after irradiation for 30 min at 10 °C. The solution was then transferred to a high pressure NMR tube and freeze-pump-thaw degassed (3X). Thirty psi of CH₃CF₃ was then introduced into the tube, which was shaken carefully at room temperature. Clean formation of **5** was observed after 1 week with trace amounts of products from activation of carbodiimide (<5%). ¹H NMR (400 MHz, C₆D₆): δ -14.344 (d, ¹J_{Rh-H} = 21.3 Hz, 1 H, RhH), 0.612 (s, 9 H, C(CH₃)₃), 2.134 (s, 3 H, pzCH₃), 2.146 (s, 3 H, pzCH₃), 2.265 (s, 3 H, pzCH₃), 2.323 (s, 3 H, pzCH₃), 2.515 (s, 3 H, pzCH₃), 2.524 (s, 3 H, pzCH₃), 2.703 (d, ⁴J_{Rh-H} = 2.2 Hz, 2 H, NCH₂), 5.530 (s, 1 H, pzH), 5.605 (s, 1 H, pzH), 5.795 (s, 1 H, pzH), signals for RhCH₂ are overlapping with those for pzCH₃ based on cross coupling in the ¹H-¹³C HSQC spectrum. ¹³C{¹H} NMR (500 MHz, C₆D₆): δ 8.31 (quint, ¹J_{Rh-C} = ²J_{F-C} = 26.9 Hz, 1 C, RhCH₂), 12.44 (s, 1 C, pz-CH₃), 12.60 (s, 1 C, pz-CH₃), 12.72 (s, 1 C, pz-CH₃), 14.28 (s, 1 C, pz-CH₃), 15.46 (s, 1 C, pz-CH₃), 15.59 (s, 1 C, pz-CH₃), 26.54 (s, 3 C, C(CH₃)₃), 31.38 (s, 1 C, C(CH₃)₃), 56.11 (s, 1 C, RhCNCH₂), 106.81 (s, 1 C, pz-H), 106.55 (s, 1 C, pz-H), 105.56 (s, 1 C, pz-H), 135.70 (q, ¹J_{F-C} = 275.0 Hz, CF₃), 143.40 (s, 1 C, pz-C), 143.61 (s, 1 C, pz-C), 143.87 (s, 1 C, pz-C), 149.34 (s, 1 C, pz-C), 149.60 (s, 1 C, pz-C), 150.55 (s, 1 C, pz-C). ¹⁹F NMR (400 MHz, C₆D₆): δ 9.278 (dt, ²J_{CH₂-F} = 15.4 Hz, ³J_{Rh-F} = 5.4 Hz, 3 F). Anal. Calcd (found) for C₂₃H₃₆BF₃N₇Rh·THF_{0.5}: C, 48.64 (48.34); H, 6.53 (6.34); N, 15.88 (15.88).

Preparation of Tp'Rh(CNneopentyl)(CH₂F)H (6). The method for preparing **6** was the same as method B for **5**, except that CH₃F was used as the gas and a longer exchange time of 1 week was required for completion. ¹H NMR (400 MHz, C₆D₆): δ -14.221 (dd, ¹J_{Rh-H} = 24.7 Hz, ³J_{F-H} = 8.6 Hz, 1 H, RhH), 0.705 (s, 9 H, C(CH₃)₃), 2.163 (s, 3 H, pz-CH₃), 2.211 (s, 3 H, pz-CH₃), 2.280 (s, 3 H, pz-CH₃), 2.378 (s, 3 H, pz-CH₃), 2.528 (s, 3 H, pz-CH₃), 2.633 (d, ⁴J_{Rh-H} = 6.9 Hz, 2 H,

NCH₂), 3.039 (s, 3 H, pz-CH₃), 5.563 (s, 1 H, pz-H), 5.667 (s, 1 H, pz-H), 5.807 (s, 1 H, pz-H), signals for RhCH₂ are overlapping with those for pzCH₃ (see spectra in SI). ¹⁹F NMR (400 MHz, C₆D₆): δ -145.30 (tdd, ³J_{Rh-H-F} = 8.6 Hz, ²J_{Rh-F} = 19.6 Hz, ²J_{CH₂-F} = 50.1 Hz, 1 F). Trace amounts of the activation products of the released carbodiimide (<5%) were also observed as well as a hydride resonance at -14.16 ppm with ¹J_{Rh-H} = 25.2 Hz. No other fluorine resonance was observed for this byproduct. This byproduct has t_{1/2} = 2.0 h in C₆D₆ at 66.9 °C, suggesting the possibility of activation of some substituted alkane, which was later confirmed by NMR and GC-MS analysis to be dimethyl ether in the commercial CH₃F. The structure for this hydride complex was therefore assigned as Tp'Rh-(CNneopentyl)(CH₂OCH₃)H (7).

Preparation of Tp'Rh(CNneopentyl)(CHF₂)H (8). The method for preparing 8 was the same as method B for 5, except that CH₂F₂ was used as the gas and a longer exchange time of 1 week was required for completion. Significant amounts of the activation products of the released carbodiimide (~71%) were also observed. ¹H NMR (400 MHz, C₆D₆): δ -14.095 (dd, ³J_{F-H} = 11.7 Hz, ¹J_{Rh-H} = 24.9 Hz, 1 H, RhH). ¹⁹F NMR (400 MHz, C₆D₆): δ -11.480 (dddd, ³J_{Rh-H-F} = 11.7 Hz, ²J_{Rh-F} = 16.1 Hz, ²J_{CH₂-F} = 54.1 Hz, ²J_{F-F} = 246.3 Hz, 1 F), -17.238 (ddd, ²J_{Rh-F} = 6.9 Hz, ²J_{CH₂-F} = 54.1 Hz, ²J_{F-F} = 246.3 Hz, 1 F).

Preparation of Tp'Rh(CNneopentyl)(CH₂C(=O)CH₃)Cl (2-Cl). A solution of 1 (50 mg, 0.073 mmol) dissolved in 1.0 mL of acetone was placed in an NMR tube sealed with a Teflon cap. This sample was irradiated for 20 min at -20 °C. The solvent was immediately removed *in vacuo* at room temperature. 1.0 mL of carbon tetrachloride was added and the solution stirred under a nitrogen atmosphere for 1 day. The volatiles were again removed and the yellow solid purified by chromatography with 5:1 hexane:THF as the eluent. Yellow crystals were collected (19.2 mg, 45%) by recrystallization in dichloromethane layered with hexane at room temperature. ¹H NMR (500 MHz, C₆D₆): δ 0.773 (s, 9 H, C(CH₃)₃), 2.059 (s, 3 H, pz-CH₃), 2.144 (s, 3 H, pz-CH₃), 2.151 (s, 3 H, pz-CH₃), 2.751 (s, 3 H, pz-CH₃), 2.798 (s, 3 H, pz-CH₃), 2.956 (s, 3 H, pz-CH₃), 2.682 (s, 3 H, COCH₃), 2.896 (d, ⁴J_{Rh-H} = 14.2 Hz, 1 H, NCH₂), 3.202 (d, ⁴J_{Rh-H} = 13.8 Hz, 1 H, NCH₂), 3.564 (dd, ²J_{Rh-H} = 6.8 Hz, ²J_{H-H} = 2.9 Hz, 1 H, RhCH₂CO), 3.975 (dd, ²J_{Rh-H} = 6.8 Hz, ²J_{H-H} = 2.9 Hz, 1 H, RhCH₂CO), 5.559 (s, 1 H, pz-H), 5.584 (s, 1 H, pz-H), 5.623 (s, 1 H, pz-H). ¹³C{¹H} NMR (500 MHz, C₆D₆): δ 12.30 (s, 1 C, pz-CH₃), 12.59 (s, 1 C, pz-CH₃), 12.80 (s, 1 C, pz-CH₃), 14.87 (s, 1 C, pz-CH₃), 15.13 (s, 1 C, pz-CH₃), 15.61 (s, 1 C, pz-CH₃), 21.11 (d, ¹J_{Rh-C} = 19.9 Hz, 1 C, RhCH₂CO), 26.78 (s, 3 C, CH₂C(CH₃)₃), 31.76 (s, 1 C, CH₂C(CH₃)₃), 34.72 (s, 1 C, CH₃), 56.88 (s, 1 C, RhCNCH₂), 108.83 (s, 1 C, pz-CH), 109.02 (s, 1 C, pz-CH), 108.19 (s, 1 C, pz-CH), 143.05 (s, 2 C, pz-C), 144.57 (s, 1 C, pz-C), 152.95 (s, 1 C, pz-C), 152.03 (s, 1 C, pz-C), 151.75 (s, 1 C, pz-C), 218.17 (s, 1 C, CO). Anal. Calcd (found) for C₂₄H₃₈N₇BOClRh·(C₆H₁₄)_{0.25}: C, 50.10 (50.27); H, 6.84 (6.68); N, 16.04 (16.07).

Preparation of Tp'Rh(CNneopentyl)(CH₂C≡CCH₃)Cl (3-Cl). A solution of 1 (50 mg, 0.073 mmol) dissolved in 1.0 mL of 2-butyne was placed in an NMR tube sealed with a Teflon cap. This sample was irradiated for 20 min at -20 °C; 1.0 mL of carbon tetrachloride was added, and the solution stirred under a nitrogen atmosphere for 1 day. The volatiles were removed under vacuum, and the yellow solid was purified by chromatography with 5:1 hexane/THF as the eluent. Red-orange crystals were collected (36.8 mg, 86%) following recrystallization from dichloromethane layered with hexane at room temperature. ¹H NMR (500 MHz, C₆D₆): δ 0.691 (s, 9 H, C(CH₃)₃), 1.294 (t, 3 H, C≡CCH₃), 2.107 (s, 3 H, pz-CH₃), 2.147 (s, 3 H, pz-CH₃), 2.223 (s, 3 H, pz-CH₃), 2.563 (s, 3 H, pz-CH₃), 2.669 (d, ⁴J_{Rh-H} = 2.6 Hz, 1 H, NCH₂), 2.782 (s, 3 H, pz-CH₃), 3.070 (s, 3 H, pz-CH₃), 3.763 (dq, ⁴J_{Rh-H} = 13.5 Hz, ³J_{H-H} = 2.7 Hz, 1 H, RhCH₂C≡C), 4.038 (dq, ²J_{Rh-H} = 13.5 Hz, ²J_{H-H} = 2.9 Hz, 1 H, RhCH₂C≡C), 5.573 (s, 1 H, pz-H), 5.660 (s, 1 H, pz-H), 5.711 (s, 1 H, pz-H). ¹³C{¹H} NMR (500 MHz, C₆D₆): δ -3.21 (d, ¹J_{Rh-C} = 19.0 Hz, RhCH₂), 4.92 (s, CH₃), 12.27 (s, 1 C, pz-CH₃), 12.74 (s, 1 C, pz-CH₃), 12.97 (s, 1 C, pz-CH₃), 14.41 (s, 1 C, pz-CH₃), 14.72 (s, 1 C, pz-CH₃), 14.82 (s, 1 C, pz-CH₃),

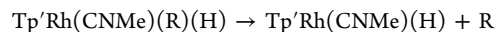
26.50 (s, 3 C, CH₂C(CH₃)₃), 31.80 (s, 1 C, CH₂C(CH₃)₃), 56.20 (s, 1 C, RhCNCH₂), 74.78 (s, RhCH₂CC), 88.91 (s, RhCH₂CC), 106.89 (s, 1 C, pz-H), 107.55 (s, 1 C, pz-H), 108.39 (s, 1 C, pz-H), 142.47 (s, 2 C, pz-C), 142.76 (s, 1 C, pz-C), 144.01 (s, 1 C, pz-C), 151.40 (s, 1 C, pz-C), 151.44 (s, 1 C, pz-C), 153.44 (s, 1 C, pz-C). Anal. Calcd (found) for C₂₅H₃₈BClN₇Rh: C, 51.26 (49.70); H, 6.54 (6.43); N, 16.74 (15.52).

Preparation of Tp'Rh(CNneopentyl)(CH₂O-t-Bu)Cl (4-Cl). A solution of 1 (50 mg, 0.073 mmol) dissolved in 0.5 mL of methyl *tert*-butyl ether was placed in an NMR tube sealed with a Teflon cap. This sample was irradiated for 30 min at -20 °C; 1.0 mL of carbon tetrachloride was added and the solution stirred under a nitrogen atmosphere for 1 day. The volatiles were removed under vacuum, and the yellow solid was purified by chromatography with 5:1 hexane/THF as the eluent. Yellow crystals were collected (21.0 mg, 46%) by recrystallization in dichloromethane layered with hexane at room temperature. ¹H NMR (500 MHz, C₆D₆): δ 0.761 (s, 9 H, C(CH₃)₃), 1.398 (s, 9 H, O-C(CH₃)₃), 2.132 (s, 3 H, pz-CH₃), 2.153 (s, 3 H, pz-CH₃), 2.244 (s, 3 H, pz-CH₃), 2.655 (s, 3 H, pz-CH₃), 2.767 (d, ²J_{H-H} = 10.6 Hz, 2 H, NCH₂), 2.814 (s, 3 H, pz-CH₃), 2.958 (s, 3 H, pz-CH₃), 5.268 (dd, ²J_{Rh-H} = 0.8 Hz, ²J_{H-H} = 3.4 Hz, 1 H, RhCH₂O), 6.386 (dd, ²J_{Rh-H} = 0.4 Hz, ²J_{H-H} = 3.4 Hz, 1 H, RhCH₂O), 5.506 (s, 1 H, pz-H), 5.687 (s, 1 H, pz-H), 5.726 (s, 1 H, pz-H). ¹³C NMR (500 MHz, C₆D₆): δ 12.30 (s, 1 C, pz-CH₃), 12.75 (s, 1 C, pz-CH₃), 12.94 (s, 1 C, pz-CH₃), 14.49 (s, 1 C, pz-CH₃), 14.51 (s, 1 C, pz-CH₃), 14.67 (s, 1 C, pz-CH₃), 26.84 (s, 3 C, CH₂C(CH₃)₃), 28.44 (s, 3 C, OC(CH₃)₃), 31.91 (s, 1 C, CH₂C(CH₃)₃), 56.11 (s, 1 C, RhCNCH₂), 57.88 (d, ¹J_{Rh-C} = 20.6 Hz, 1 C, RhCH₂O), 73.94 (s, 1 C, OC(CH₃)₃), 106.60 (s, 1 C, pz-H), 107.67 (s, 1 C, pz-H), 108.73 (s, 1 C, pz-H), 142.53 (s, 1 C, pz-C), 142.86 (s, 1 C, pz-C), 144.23 (s, 1 C, pz-C), 151.12 (s, 1 C, pz-C), 152.03 (s, 1 C, pz-C), 152.71 (s, 1 C, pz-C). Anal. Calcd (found) for C₂₆H₄₄N₇BClRh·(C₆H₁₄)_{0.25}: C, 51.50 (51.55); H, 7.46 (7.53); N, 15.29 (15.41).

Solution and Refinement of Crystal Structures for 2-Cl and 4-Cl. *Tp'Rh(CNneopentyl)(CH₂C(=O)CH₃)Cl (2-Cl).* A well-formed crystal with approximate dimensions of 0.18 × 0.14 × 0.04 mm³ was mounted on a glass fiber and placed on a Bruker SMART APEX II CCD Platform diffractometer under a cold stream of nitrogen at -173 °C. The lattice constraints were obtained from 53,344 reflections with values of *c* between 1.73 and 33.14°. Cell reduction revealed a monoclinic crystal system. Data were collected in accord with the parameters in the SI. The space group was assigned as *P2₁/n* on the basis of systematic absences and intensity statistics. The structure was solved using SIR97 and refined using SHELXS-97. All non-hydrogen atoms were refined with anisotropic displacement parameters. All hydrogen atoms were placed in ideal positions and refined as riding atoms with relative isotropic displacement parameters.

Tp'Rh(CNneopentyl)(CH₂O-t-Bu)Cl (4-Cl). A well-formed crystal with approximate dimensions of 0.20 × 0.16 × 0.05 mm³ was mounted on a glass fiber and placed on a Bruker SMART APEX II CCD platform diffractometer under a cold stream of nitrogen at -173 °C. Final cell constants were calculated from the *xyz* centroids of 3525 strong reflections from the actual data collection after integration. Cell reduction revealed a monoclinic crystal system. Data were collected in accord with the parameters in the SI. The space group was assigned as *Cc* on the basis of systematic absences and intensity statistics. The structure was solved using SHELXS-97 and refined using SHELXL-97. All non-hydrogen atoms were refined with anisotropic displacement parameters. All hydrogen atoms were placed in ideal positions and refined as riding atoms with relative isotropic displacement parameters.

Calculation of C-H and Relative Rh-C Bond Strengths. Bond dissociation energies were calculated as the reaction:



The only simplification used during calculations was replacing neopentyl isocyanide with methyl isocyanide. We have previously shown this simplification to have no discernible effect (see ref 23 for details on the choice of method). Gas-phase structures were calculated using unrestricted DFT with the M06-2x functional. Calculations were done using the Gaussian09 package. Light atoms (H through F) were

modeled with the 6-31G** basis set. Heavy atoms (Rh, Cl) were modeled with ECP pseudopotentials of the Stuttgart group and the basis sets further augmented with d or f polarization functions that have been optimized by Frenking (Rh $\alpha = 1.350$; Cl $\alpha = 0.640$). Geometries were optimized without constraints. Frequency calculations were done to check for local minima. Free energies were calculated at 298.15 K and 1 atm.

X-ray crystallographic data have been deposited as CCDC deposition nos. 919108 and 919109.

■ ASSOCIATED CONTENT

📄 Supporting Information

Tables of NMR data, kinetic data, X-ray crystallographic data as CIF files, coordinates and energies for calculated complexes, a summary of the calculation procedure. This material is available free of charge via the Internet at <http://pubs.acs.org>.

■ AUTHOR INFORMATION

Corresponding Author

jones@chem.rochester.edu

Notes

The authors declare no competing financial interest.

■ ACKNOWLEDGMENTS

We acknowledge the U.S. Department of Energy (Grant DE-FG02-86ER13569) for their support of this work. We acknowledge the Center for Integrated Research Computing at the University of Rochester for providing the necessary computing systems and personnel to enable the research presented in this manuscript.

■ REFERENCES

- (1) Pruett, R. L. *Adv. Organomet. Chem.* **1979**, *14*, 1.
- (2) Bini, L.; Müller, C.; Vogt, D. *ChemCatChem* **2010**, *2*, 590.
- (3) Schwartz, J.; Labinger, J. A. *Angew. Chem., Int. Ed. Engl.* **1976**, *15*, 333.
- (4) Tamaki, A.; Kochi, J. K. *J. Chem. Soc., Chem. Commun.* **1973**, 423.
- (5) Reger, D. L.; Culbertson, E. C. *Inorg. Chem.* **1977**, *16*, 3104.
- (6) Reger, D. L.; Garza, D. G.; Lebioda, L. *Organometallics* **1992**, *11*, 4285.
- (7) Reger, D. L.; Garza, D. G.; Baxter, J. C. *Organometallics* **1990**, *9*, 873.
- (8) (a) Janowicz, A. H.; Bergman, R. G. *J. Am. Chem. Soc.* **1983**, *105*, 3929. (b) Buchanan, J. M.; Stryker, J. M.; Bergman, R. G. *J. Am. Chem. Soc.* **1986**, *108*, 1537.
- (9) Northcutt, T. O.; Wick, D. D.; Vetter, A. J.; Jones, W. D. *J. Am. Chem. Soc.* **2001**, *123*, 7257.
- (10) Chirik, P. J.; Day, M. W.; Labinger, J. A.; Bercaw, J. E. *J. Am. Chem. Soc.* **1999**, *121*, 10308.
- (11) (a) Craig, P. J.; Green, M. J. *Chem. Soc. (A)* **1968**, 1978. (b) Wojcicki, A. *Adv. Organomet. Chem.* **1973**, *11*, 87.
- (12) Hartwig, J. F. Selected Reactions of Metal-Alkyl Complexes. In *Organotransition Metal Chemistry: From Bonding to Catalysis*; University Science Books: Sausalito, 2010; Chapter 3, (3.2.1.4), p 90.
- (13) Reger, D. L.; McElligott, P. J. *J. Organomet. Chem.* **1981**, *216*, C12.
- (14) Harvey, J. N. *Organometallics* **2001**, *20*, 4887.
- (15) Vela, J.; Vaddadi, S.; Cundari, T. R.; Smith, J. M.; Gregory, E. A.; Lachicotte, R. J.; Flashenriem, C. J.; Holland, P. L. *Organometallics* **2004**, *23*, 5226.
- (16) Aeby, A.; Consiglio, G. *Dalton Trans.* **1999**, 655.
- (17) Brookhart, M.; Rix, F. C.; Desimone, J. M.; Barborak, J. C. *J. Am. Chem. Soc.* **1992**, *114*, 5894.
- (18) Pellecchia, C.; Pappalardo, D.; Oliva, L.; Zambelli, A. *J. Am. Chem. Soc.* **1995**, *117*, 6593.
- (19) (a) Jones, W. D.; Hessel, E. T. *J. Am. Chem. Soc.* **1993**, *115*, 554. (b) Jones, W. D.; Wick, D. D. *Organometallics* **1999**, *18*, 495.
- (20) (a) Vetter, A. J.; Jones, W. D. *Polyhedron* **2004**, *23*, 413. (b) Vetter, A. J.; Rieth, R. D.; Brennessel, W. W.; Jones, W. D. *J. Am. Chem. Soc.* **2009**, *131*, 10742.
- (21) Vetter, A. J.; Rieth, R. D.; Jones, W. D. *Proc. Natl. Acad. Sci. U.S.A.* **2007**, *104*, 6957.
- (22) Evans, M. E.; Li, T.; Vetter, A. J.; Rieth, R. D.; Jones, W. D. *J. Org. Chem.* **2009**, *74*, 6907.
- (23) Choi, G.; Morris, J.; Brennessel, W. W.; Jones, W. D. *J. Am. Chem. Soc.* **2012**, *134*, 9276.
- (24) Evans, M. E.; Burke, C. L.; Yaibuathes, S.; Clot, E.; Eisenstein, O.; Jones, W. D. *J. Am. Chem. Soc.* **2009**, *131*, 13464.
- (25) Hessel, E. T.; Jones, W. D. *Organometallics* **1992**, *11*, 1496.
- (26) Wick, D. D.; Northcutt, T. O.; Lachicotte, R. J.; Jones, W. D. *Organometallics* **1998**, *17*, 4484.
- (27) Vetter, A. J.; Flaschenriem, C.; Jones, W. D. *J. Am. Chem. Soc.* **2005**, *127*, 12315.
- (28) Jones, W. D.; Hessel, E. T. *J. Am. Chem. Soc.* **1992**, *114*, 6087.
- (29) For a discussion of this statement, see: Wilkinson, G. *Pure Appl. Chem.* **1972**, *30*, 627.
- (30) Note that earlier published calculations (refs 23 24) did not take into account that the ΔG^\ddagger for reductive elimination of the substrate RH was measured at a different temperature than the ΔG^\ddagger for reductive elimination of benzene (298 K).
- (31) Siegbahn, P. E. M. *J. Phys. Chem.* **1995**, *99*, 12723.
- (32) (a) Clot, E.; Besora, M.; Maseras, F.; Mégret, C.; Eisenstein, O.; Oelckers, B.; Perutz, R. N. *Chem. Commun.* **2003**, 490. (b) Clot, E.; Oelckers, B.; Klahn, A. H.; Eisenstein, O.; Perutz, R. N. *Dalton Trans.* **2003**, 4065. (c) Clot, E.; Mégret, C.; Eisenstein, O.; Perutz, R. N. *J. Am. Chem. Soc.* **2009**, *131*, 7817.
- (33) Siegbahn, P. E. M. *J. Am. Chem. Soc.* **1994**, *116*, 7722.
- (34) Sakaki, S.; Biswas, B.; Sugimoto, M. *Organometallics* **1998**, *17*, 1278.
- (35) Bryndza, H. E.; Fong, L. K.; Paciello, R. A.; Tam, W.; Bercaw, J. E. *J. Am. Chem. Soc.* **1987**, *109*, 1444.
- (36) (a) Bennett, J. L.; Wolczanski, P. T. *J. Am. Chem. Soc.* **1994**, *116*, 2179. (b) Bennett, J. L.; Wolczanski, P. T. *J. Am. Chem. Soc.* **1997**, *119*, 10696.
- (37) Clot, E.; Mégret, C.; Eisenstein, O.; Perutz, R. N. *J. Am. Chem. Soc.* **2006**, *128*, 8350.
- (38) Uddin, J.; Morales, C. M.; Maynard, J. H.; Landis, C. R. *Organometallics* **2006**, *25*, 5566.